Inorganica Chimica Acta 466 (2017) 612–617

Contents lists available at ScienceDirect

Inorganica Chimica Acta

journal homepage: www.elsevier.com/locate/ica

Research paper

Synthesis, characterization and liquid crystalline properties of novel benzimidazol-8-hydroxyquinoline complexes

Taghreed H. Al-Noor [a], Nisreen H. Karam [a], Faeza H. Ghanim [a], Alia S. Kindeel [a], Ammar H. Al-Dujaili [b,*]

[a] Department of Chemistry, College of Education for Pure Science, Ibn Al- Haitham, University of Baghdad, Baghdad, Iraq
[b] Hamdi Mango Center for Scientific Research, University of Jordan, Amman, Jordan

ARTICLE INFO

Article history:
Received 27 May 2017
Received in revised form 11 July 2017
Accepted 12 July 2017
Available online 18 July 2017

Keywords:
Benzimidazol
Liquid crystal
Metal heterocyclic
8-Hydroxyquinoline
Transition metal-complexes

ABSTRACT

The synthesis, characterization and liquid crystalline properties of N4,N4′-bis((1 H-benzo[*d*]imidazol-2-yl)methyl)-3,3′-dimethyl-[1,1′-biphenyl]-4,4′-diamine and of their corresponding Mn(II), Fe(II), Ni (II), Cu(II), and Zn(II) complexes are described. The ligand and complexes have been characterized by elemental analysis, magnetic susceptibility measurements (μeff), conductometric measurements and Fourier Transform Infrared (FTIR), Nuclear Magnetic Resonance (^{1}H NMR), (^{13}C-NMR) and UV–Vis spectroscopy. Spectral investigations suggested octahedral coordination geometrical arrangement for M(II) complexes. The phase transition temperatures were detected by differential scanning calorimetry (DSC) analysis and the phases are confirmed by optical polarizing microscopy (POM). The DSC and POM supported the mesomorphic properties of the uncoordinated ligand in which the enantiotropic smectic phases were recorded. However, not all of their corresponding M(II) complexes are liquid crystal.

1. Introduction

A liquid crystalline mesophase is a state of matter intermediate between liquid and solid. Benzimidazoles are an important class of heterocyclic that used in many applications includes their use as liquid crystal complexes [1], polymers [2] and organic ligands [3,4]. The classical and most common methods to assemble benzimidazoles or bisbenzimidazole derivatives involve the condensation of benzene-1,2-diamines with aldehydes, carboxylic acids, or their derivatives under strong acid/high temperature conditions or by using a stoichiometric oxidant [5,6].

Several liquid crystalline compounds and complexes containing benzimidazoles have been synthesized and well studied. For example, Ninán et al. [7] synthesized and studied mesomorphic properties of 2-pentadecylbenzimidazole and 1,1′-bis(octadecyl)-2,2′-bibenzimidazole. The former compound exhibit an enantiotropic smectic C (SmC) phase, whereas the later compound exhibit a monotropic cholesteric phase. These two compounds represent the first benzimidazole-based liquid crystals. The synthesis, characterization and mesomorphic properties of a series of N-(2-hydroxy-4-*n*-alkyloxybenzylidene) 4′-amino-2-methylbutylcinnamate and their copper (II) complexes are reported [8]. The imines exhibited smectic A (SmA) and chiral SmC phases while their copper (II) complexes displayed SmA–SmC phase variant. Tan et al. [9] synthesized a homologous series of biphenyl benzoate-based compounds with an alkylthio chain bearing a benzimidazole moiety as a terminal substituent. The compounds exhibited SmA and nematic phases over a temperature range of 173–116 °C during the cooling process. Recently [10], three series of 2-(4_-alkoxybiphenyl-4-yl)-1*H*-benzimidazole derivatives, which possessed 5-nitrobenzimidazole, benzimidazole or 5-methylbenzimidazole units at the end of the molecule, were synthesized. All the compounds exhibited enantiotropic smectic mesophases with wide temperature domains for a carbon number in the alkoxy chain from 6 to 16.

Liquid crystalline materials containing metal ions are known as metallomesogens [11–13]. The interest on studying of these systems arises from the fact that the combination of the properties of organic liquid crystals and of transition-metal ions can produce new materials exhibiting unique assembly structures, and unique optical, magnetic and electronic properties [14–20]. Moreover, due to the various oxidation states and the array of coordination geometries, 4–6 metal ions offer many possibilities as building blocks for unique molecular structures when associated with suitably designed ligands. Metal ions, for example, Ni(II), Cu(II), Pd(II) or Pt(II) with square-planar coordination were commonly used [21].

During the last decade many series of metallomesogens have been synthesized. Among these metallomesogens containing benzimidazole or 8-hydroxyquinoline derivatives have been studied as excellent candidates for material applications due to their excellent thermal and chemical stabilities and electroptics

* Corresponding author.
E-mail address: ah.aldujaili@gmail.com (A.H. Al-Dujaili).

http://dx.doi.org/10.1016/j.ica.2017.07.029
0020-1693/

properties. For example, a new series of star-shaped iron (II) spin crossover (SCO) complexes based on symmetric tripod, 1-alkyl-1*H*-imidazole and 1-alkyl-1*H*-benzimidazole ligands with variable-length alkyl chains were reported, long chain species display SCO and liquid crystal properties [22]. Pucci et al. [23] synthesized the first gallium(III)-based liquid crystal by grafting around the metal centre two chelating 2-methylquinolin-8-olate anions and one monodentate 3,4,5-tris- (hexadecyloxy)benzoyloxy ligand, allowing the resulting complex to be a soft luminescent material with the typical high quantum yield of penta coordinated gallium species.

In this work, we report the synthesis, characterization and mesomorphic behavior of Mn(II), Fe(II), Ni (II), Cu(II), and Zn(II) complexes of ligand containing benzimidazole-8-hydroxyquinoline unit. The liquid crystalline behavior has been analyzed in terms of structural property relationship between metal centers and ligands. Because, this relationship can be used to control the mesomorphism of the complexes formed.

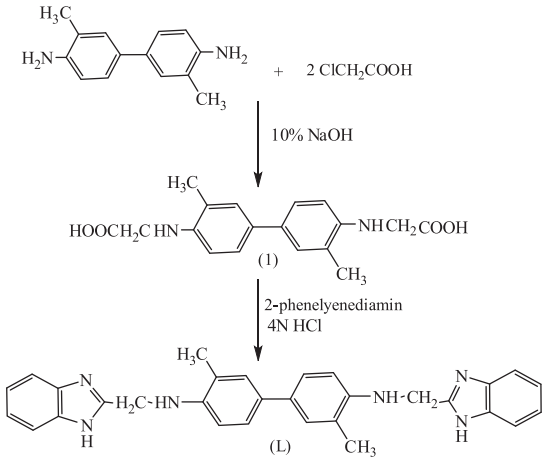

N4,N4'-bis((1H-benzo[d]imidazol-2-yl)methyl)-3,3'-dimethyl-[1,1'-biphenyl]-4,4'-diamine (L)

Scheme 1. The synthesis route of the ligand (L).

2. Experimental

2.1. Chemicals

All chemicals were of reagent grade obtained from Sigma-Aldrich Chemicals and used as received.

2.2. Techniques

Infrared spectra were recorded on a Shimadzu 8000 FTIR spectrophotometer in the wave number range 4000–400 cm^{-1} using KBr discs or films. ^{1}H- and ^{13}C-NMR spectra were obtained with Avance III Bruker 500 MHz instrument using tetramethylsilane (TMS) as the internal standard. Conductivities were measured for 10^{-3} M of complexes in (DMSO) at 25 °C using (Philips PW- Digital Conduct meter). UV–Vis spectra were recorded on a (Shimadzu UV-160 A) Ultra Violet-Visible spectrophotometer. Uncorrected melting points were determined by using Hot-Stage, Gallen Kamp melting point apparatus. The concentration of metal was measured by using Flame Atomic Absorption Spectrometer (FAAS, Perkin-Elmer 400, UK) using air and acetylene as flame gases.

The optical behavior observations were made using polarized optical microscope (POM) model Leica DM2500M with a Leitz Laborlux 12 Pols hot stage and PR600 controller. Photographs of texture were obtained using a camera model PM-10AD made Olympus. The transition temperatures and enthalpies were investigated using differential scanning calorimetry DSC (STA PT-1000LINSIS), ramp rate: 10 degree centigrade per minute under nitrogen atmosphere. Temperature and heat flow calibrated with standard indium of purity > 99.99%.

2.3. Synthesis

The synthesis of the compound (1) and ligand (L) were accomplished by the reaction sequences outlined in Scheme 1.

2.3.1. Synthesis of 2,2′-(3,3′-dimethylbiphenyl-4,4′-iyl)bis (azanediyl)diacetic acid (1)

To a stirring of α-chloroacetic acid (1.89 g, 20 mmol) in 10% aqueous sodium hydroxide 10 mL, a solution of 3,3′-dimethylbiphenyl-4,4′-diamine (2.12 g, 10 mmol) in 10% aqueous solution of sodium hydroxide 10 mL was added, the mixture was refluxed for three hours. After cooling, the solution was acidified with concentrated hydrochloric acid. The precipitate was filtered and recrystallized from ethanol.

Orange solid. Yield: 75%. m.p.: 82-85 °C. FT-IR (KBr, cm^{-1}): 3410 (ν_{O-H}); 3213 ($\nu_{sym,asym,N-H}$); 3093 (ν_{Ar-H}); 1722 ($\nu_{C=O}$). ^{1}H NMR (DMSO-d_6), ppm: δ = 11.38 (s, 2H, COOH); 7.05–8.00 (dd, 6H, CHAr); 4.15 (s, 4H, CH_2); 5.64 (s, 2H, NH); 2.15 (s, 6H, CH_3). ^{13}C-NMR (DMSO-d_6), ppm: δ = 177.8 (COOH); 127.8–156.9 (C-aromatic); 32.3 (CH_2); 21.2 (CH_3). Anal. Calc. for $C_{18}H_{20}O_4N_2$: C, 65.85; H, 6.10; N, 8.54.. Found: C, 66.12; H, 5.98; N, 9.11.

2.3.2. Synthesis of N4,N4′-bis((1H-benzo[d]imidazol-2-yl)methyl)-3,3′-dimethylbiphenyl-4,4′-diamine (L)

A mixture of compound (1) (3.28 g, 10 mmol) and 2-phenylenediamine (2.16 g, 20 mmol) in 4 N hydrochloric acid (40 mL) was refluxed for 10 h. Then the solution was neutralized with ammonia to precipitate benzimidazole (Scheme 1). The product was filtered and recrystallized from acetone.

Dark brown solid. Yield: 60%. m.p.: 118-123 °C. FT-IR (KBr, cm^{-1}): 3368 ($\nu_{sym,asym,N-H}$); 3057 (ν_{CH-Ar}); 2852 ($\nu_{CH-aliphatic}$); 1618 ($\nu_{C=N\ bezimidazole}$); 1578 ($\nu_{C=C}$); 1111 (ν_{CH-Ar}). ^{1}H NMR (DMSO-d_6), ppm: δ = 12.21 (s, 2H, NH for benzimidazol rings); 6.29–7.89 (dd, 14H, CHAr); 5.48 (s, 2H, NH); 4.93 (s, 4H, CH_2); 2.10 (s, 6H, CH_3). ^{13}C-NMR (DMSO-d_6), ppm: δ = 114.1–158.7 (C-aromatic); 46.2 (CH_2); 18.2 (CH_3). Anal. Calc. for $C_{30}H_{26}N_6$: C, 76.27; H, 5.51; N, 17.80.. Found: C, 76.89; H, 5.11; N, 18.21.

2.3.3. Synthesis of metal complexes [$M_2(L)(Q)_4$] M = Mn(II), Fe(II), Ni(II), Cu(II), and Zn(II) sodiumoxyqinolinate

The reaction sequences leading to the formation of metal complexes [$M_2(L)(Q)_4$] are outlined in Scheme 2.

Sodium-8-oxyqinolinate (Q) was synthesized by the reaction of 8-hydroxyquinoline (0.58 g, 4 mmol) with sodium hydroxide (0.16 g, 4 mmol) in ethanol. The mono ligand complexes were synthesized by the reactions of ethanolic solutions of metal chlorides with ligand in a 1: 2 (M: L) mole ratio by raising the pH to 6.0–6.5 with a 5% aqueous sodium hydroxide solution and stirring the solution on a magnetic stirrer at 20–60 °C. The pH was controlled with the aid of pH paper and stirring was continued for thirty minutes. The complexes separated out, filtered and washed two times with (50% ethanol: water). All the complexes are colored powders. The complexes are stable in air and insoluble in water but soluble in chloroform, acetone, ethanol, methanol and benzene and very soluble in dimethylsulfoxide (DMSO) and dimethylformamide (DMF).

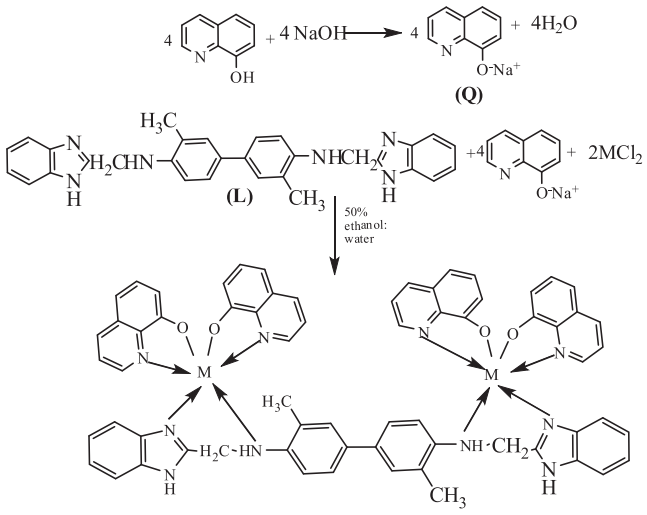

Scheme 2. The Synthesis route of $[M_2(L)(Q)_4]$ complexes.

3. Results and discussion

3.1. Characterization of (1) and (L)

The dicarboxylic acid (1) was synthesized by the reaction of one mole of 3,3′-dimethylbiphenyl-4,4′-diamine (o-tolidin) with two moles of α-chloro acetic acid by neucleophilic addition reaction in 10% aqueous NaOH solution. The ligand (L), N4,N4′-bis((1H-benzo [*d*]imidazol-2-yl)methyl)-3,3′-dimethylbiphenyl-4,4′-diamine was synthesized by the cyclization of compound (1) with two moles of 2-phenylenediamine in 4N hydrochloric acid followed by neutralized with ammonia. The structure of these two compounds were characterized by elemental analysis, FTIR, ^{1}H NMR and ^{13}C-NMR spectroscopy. The percentages of C, H and N from the elemental analysis were in good agreement with the calculated values for compounds (1) and (L).

The FTIR spectrum of compound (1) showed disappearance absorption stretching bands of NH_2 groups for starting material o-tolidin and appearance stretching bands of carboxyl and hydroxyl groups for dicarboxylic acid. The FTIR spectrum of ligand (L) showed absorption stretching bands of C=N groups for benzimidazole ring [24] and disappearance stretching bands of carboxyl and hydroxyl groups for dicarboxylic acid (1). The sharp peak at 3368 (strong) cm^{-1} was observed and assigned to the absorption band of NH in the benzimidazole moiety which indicated that the NH group was associated with N atom via intermolecular N-H–N hydrogen bonding [25].

The ^{1}H NMR spectrum for ligand (L) showed a signal at δ 2.10 ppm due to six protons of two CH_3 groups, a signal at δ 4.93 ppm for four protons of two CH_2 groups, while a signal at δ 5.48 ppm may be assigned to two protons of NH groups. Many signals in the region δ = 6.29–7.89 ppm that could be attributed to fourteen protons of aromatic rings. A signal at δ = 12.21 ppm can be attributed to two protons of NH for benzimidazole rings [26]. The ^{13}C-NMR spectrum of compounds of ligand (L) showed the following signals: δ = 114.1–158.7 (C-aromatic); 46.2 (CH_2); 18.2 (CH_3). The data of FTIR, ^{1}H NMR and ^{13}C-NMR spectrum along with elemental analyses data confirmed the structural formula of the synthesized compounds.

3.2. Characterization of mixed ligands metal complexes

Generally, the complexes were synthesized by reacting the respective metal chloride with the ligands (L) and (Q) using 2:1:4 mol ratio, i.e., two moles of metal chloride: one mole of ligand (L) and four moles of sodiumoxyqinolinate (Q). The formula weights and melting points are given in Table 1 based on the physicochemical characteristics. The complexes were analyzed for their metal percentage by Flame-AAS. All complexes gave approximated values and they were consisted with theoretical values.

The FTIR spectrum for the complexes exhibit new bands at 486, 478, 451, 478 and 459 cm^{-1} were assigned to υ_{M-O} for complexes $[Mn_2(L)(Q)_4]$, $[Fe_2(L)(Q)_4]$, $[Ni_2(L)(Q)_4]$, $[Cu_2(L)(Q)_4]$ and $[Zn_2(L)(Q)_4]$, respectively, indicating that the oxygen of (Q^-) is involved in coordination with metal ions. The FTIR spectra contained the bands at 1618–1632 cm^{-1}, $\upsilon_{C=N\text{benzimidazole ring}}$, of the two ligands were shifted slightly to a higher value in all the complexes suggesting that the ligands are coordinated through -C=N- [27,28]. However, free secondary NH group exhibit N-H stretching frequencies in the 3300–3500 cm^{-1} region which are shifted by about 100–200 cm^{-1} wave number after coordination with a metal ion in ligand (L) observed at 3236 cm^{-1} shifted at range 3364–3394 cm^{-1} [29]. The absorption due to Ar-C-CH_3 group did not change in the spectra of complexes indicating that Ar-C-CH_3 groups is not involved in coordination with the M(II). The absorption stretching band $\nu_{C=N}$ that occur at 1618 cm^{-1} in the free ligand (L) shifted to lower frequencies in all the complexes confirming that the M(II) are coordinated directly to the benzimidazole (N) atom. Also strong υ_{C-O} phenolic band observed at 1418 cm^{-1} indicates the presence of oxine (Q^-) moiety in the complexes shifted to higher frequencies in all the complexes confirming that the M(II) are coordinated through its (O) atom bidentate ligand [28–30].

The electronic spectral data of the free ligands, (L) and (Q) and their complexes are measured in DMSO solution between 200 and 1100 nm at room temperature together with the magnetic susceptibility (μeff). For the all complexes the μeff were found to be paramagnetic in nature except $[Zn_2(L)(Q)_4]$ complex. The UV– Vis spectra for the (Q) and ligand (L), exhibit absorption peaks at UV–vis (λ: nm) (ε: L mol^{-1} cm^{-1}): (275) (36,363), (325) (30769), (270) (37,037) and (323) (30,959), which have their origin in the ($\pi \rightarrow \pi^*$) and ($n \rightarrow \pi^*$) transitions, respectively within the organic ligand [31,32].

The UV–Vis spectrum of $[Mn_2(L)(Q)_4]$ exhibits four peaks, the first and second high intense peaks at (269) (37,174) and (342) (29,239) are due to the ligand field (L.F) and charge transfer (C.T) transitions, respectively. The third and fourth absorption bands related to (d-d) transitions at (403) (24,813) and (807) (12,391 cm^{-1}), are due to the ($^6A_1g \rightarrow {}^4T_1)\upsilon_3$ and ($^6A_1g \rightarrow {}^4T_2g$, $^6A_1g)\upsilon_2$, respectively and μ_{eff} equal to 4.48 B.M, which suggests octahedral geometry around the central metal ion [31,32].

The UV–Vis spectrum of $[Fe_2(L)(Q)_4]$ exhibits five peaks. The first peak at (270) (37,037) is due to the (L.F) transition and the second, third high intense peaks at (362, 373) (29,239) are due to the (C.T) transition, the last two weak peaks at (463–579) assigned to (d–d) transition including $^5T_2g \rightarrow {}^5Eg$ transitions [31,32].

The UV–Vis spectrum of $[Ni_2(L)(Q)_4]$ exhibits five peaks. The first peak at (270) (37,037) is due to the (L.F) transition and second high intense peaks at (342) (29,239) is due to the (C.T) transition, the last three weak peaks at (860) (11,627), (584) (18,248) and (355) (28,196) assigned to (d–d) transition including $^3A_2g^{(F)} \rightarrow {}^3T_2g^{(F)}$ (υ_1), $^3A_2g^{(F)} \rightarrow {}^3T_1g^{(F)}$ (υ_2) and $^3A_2g^{(F)} \rightarrow {}^3T_1g^{(p)}(\upsilon_3)$. The complex exhibits a value of μ_{eff} = 2.26 B.M, which suggests an octahedral geometry around the central metal ion [30,31]. The

Table 1
The Physical properties and metal% of complexes.

Complex	M.Wt. (g/mol)	Colour	Yield%	M.P. (°C)	Conductivity (Ω^{-1} cm^2 mol^{-1})	Metal% Calcd. (Found)
$[Mn_2(L)(Q)_4]$	1158.67	Pale brown	67	280 (dec.)	13.11	9.84 (9.01)
$[Fe_2(L)(Q)_4]$	1160.49	Dark brown	85	280 (dec.)	6.93	9.63 (9.15)
$[Ni_2(L)(Q)_4]$	1166.22	Green	82	280 (dec.)	6.50	10.07 (9.57)
$[Cu_2(L)(Q)_4]$	1175.88	Green	77	82	5.34	10.81 (10.36)
$[Zn_2(L)(Q)_4]$	1179.56	Yellow	89	326	13.14	11.09 (10.66)

spectral parameters of the Ni(II) complex are as follows: υ_1/υ_2 ratio is 0.637, Dq = 11627 cm^{-1}, the υ_2/υ_1 ratio is 1.56, which is in the usual range reported for an octahedral Ni(II) complexes [31].

The $[Cu_2(L)(Q)_4]$ complex exhibit three peaks. the first peak at (270) (37,037) is due to the (L.F) transition and second high intense peaks at (334) (29,940) is due to the (C.T) transition, and broad band centered at (422) (23,696) due to $^2Eg \rightarrow {}^2T_2g$ transition [32].

The diamagnetic $[Zn_2(L)(Q)_4]$ complex exhibits band at (337) (29,673) for the (C.T) transition and absence of any (d-d transition) consequently, this confirms the presence of an octahedral geometry in the Zn (II) complex [33].

3.3. Mesomorphic properties

The liquid crystalline properties for the synthesized compounds were investigated using DSC and POM. The phase transition temperatures and corresponding enthalpy changes for compound (1), ligands (L) and complexes $[M_2(L)(Q)_4]$ were summarized in Table 2. The thermal behavior obtained by DSC is consistent with the data observed by POM, where it was possible to identify the mesomorphic character of the mesophases. On heating, the first endothermic peak is accompanied with high enthalpy indicates a transition from solid crystalline state to a liquid crystalline mesophase. The second endothermic transition at higher temperature presented lower associated enthalpy, which indicates transitions between distinct mesophases and to the isotropic state.

As shown in Table 2, compound (1) exhibited enantiotropic mesophases, two endothermic peaks at 83 °C and 147 °C corresponding to the melting and liquid crystal–isotropic phase transition phenomena during the heating process (Fig. S1). The formed mesophase showed a typical thread-like nematic texture under POM observation, as shown in Fig. 1. Compound (1) showed only nematic phase, this could be explained to the presence of terminal

Table 2
The phase transition temperatures and enthalpy changes of compound (1), ligand (L) and $[M_2(L)(Q)_4]$ complexes.

Compound	Transition temperatures (°C) (ΔH, kJ/mol)
(1)	Cr $\xrightarrow{83\,^oC\,(9.43)}$ N $\xrightarrow{147^oC\,(2.87)}$ I
(L)	Cr $\xrightarrow{120^oC\,(27.28)}$ SmC $\xrightarrow{138^oC\,(1.15)}$ I
$[Mn_2(L)(Q)_4]$	Cr $\xrightarrow{280\,^oC}$ I (dec.)
$[Fe_2(L)(Q)_4]$	Cr $\xrightarrow{280\,^oC}$ I (dec.)
$[Ni_2(L)(Q)_4]$	Cr $\xrightarrow{280\,^oC}$ I (dec.)
$[Cu_2(L)(Q)_4]$	Cr $\xrightarrow{79\,^oC\,(18.39)}$ SmA $\xrightarrow{125^oC\,(0.71)}$ I
$[Zn_2(L)(Q)_4]$	Cr $\xrightarrow{325^oC\,(12.54)}$ N $\xrightarrow{348^oC\,(3.04)}$ I

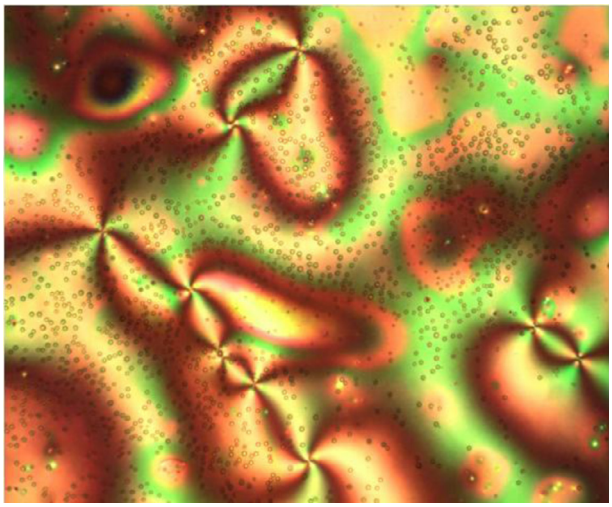

Fig. 1. Photomicrograph (×200) of compound (1) a thread-like texture of the nematic mesophase at 91 °C on heating.

dicarboxylic groups which leads to the formation of intermolecular hydrogen bonding (Scheme 3). The intermolecular hydrogen bonding leads to a lengthening of the rigid-rod moiety, which led to display nematic liquid crystalline behavior [34].

Fig. S2 shows the DSC thermogram of the ligand (L). The ligand exhibited enantiotropic mesophases during heating and cooling processes (Table 2). The liquid crystal phase type was assigned based on POM observations. Characteristic schlieren textures (Fig. 2) observed in the mesophase indicated appearance of a SmC phase. It was reported [10] that the benzimidazole moieties participated in hydrogen-bonding both as donors and acceptors and the intermolecular hydrogen-bonding formed lamellar networks in the SmC phase. The lateral intermolecular hydrogen bonding between neighboring benzimidazole moieties accounted for the interdigitated bilayer structure [25]. Similar results were reported for benzimidazole liquid crystal derivatives [7,9].

In spite of the liquid crystallinity of uncoordinated ligand (L), not all of their corresponding M(II) complexes are mesogenic. The Optical observation shows that complexes $[Mn_2(L)(Q)_4]$, $[Fe_2(L)(Q)_4]$ and $[Ni_2(L)(Q)_4]$ are non-mesogenic. These complexes have clearly melted and transformed into isotropic phase with decomposition. The TGA thermograms for these three complexes exhibit only strong broad decomposition endothermic crystal to isotropic transition (Fig. S2). The liquid crystallinity for these three complexes could be obscured by the decomposition at isotropic temperature. Complexes $[Cu_2(L)(Q)_4]$ and $[Zn_2(L)(Q)_4]$ were mesogenic and exhibited enantiotropic SmA and nematic phases, respectively. The DSC thermogram of complex $[Cu_2(L)(Q)_4]$ (Fig. S3) showed two endothermic transition on heating (Cr → SmA and SmA → I). Under optical microscope complex $[Cu_2(L)(Q)_4]$ exhibited typical focal conic fan-shaped texture of SmA, while $[Zn_2(L)(Q)_4]$ display thread-like nematic texture mesophase (Figs. 3 and 4).

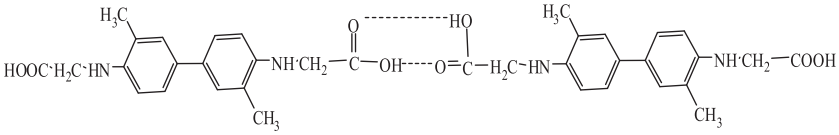

Scheme 3. Hydrogen bonding formation for compound (1).

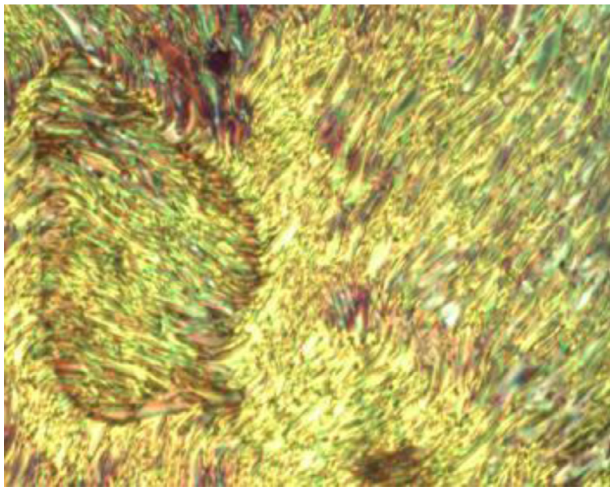

Fig. 2. Cross polarizing photomicrograph (×200) of ligand (L) schlieren texture of the smectic C (SmC) mesophase at 125 °C on heating.

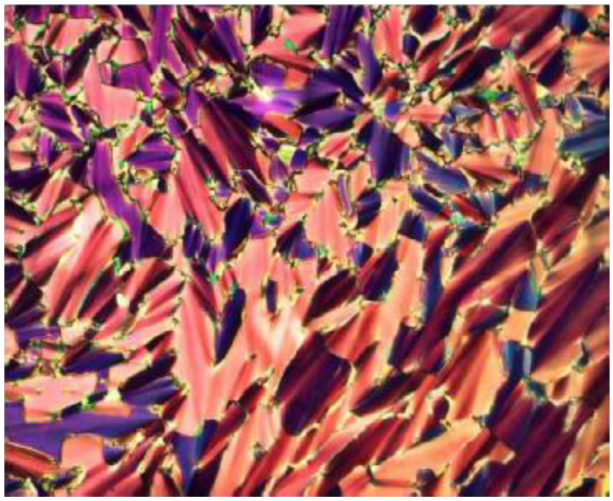

Fig. 3. Cross polarizing photomicrograph (×200) of complex $[Cu_2(L)(Q)_4]$ focal conic fan-shaped texture of the smectic A (SmA) mesophase at 84 °C on heating.

4. Conclusions

In summary, ligand (L), benzimidazole compound were synthesized and characterized. A novel $[M_2(L)(Q)_4]$ complexes were synthesized by reacted L and Q with metal(II) salts. The possible geometry of synthesized complexes is octahedral and it is six coordinated metal ligand complexes. The liquid crystalline behavior for compounds (1), ligand (L) and all complexes were examined. The compound (1) showed enantiotropic nematic mesophase while the ligand (L) displays enantiotropic SmC mesophase. The formation of SmC mesophase was attributed to the lateral intermolecular hydrogen bonds resulting from benzimidazole groups of the ligand. The novel complexes $[Cu_2(L)(Q)_4]$ and $[Zn_2(L)(Q)_4]$ exhibit a mesomorphism behavior, nematic and SmA mesophases, but the others

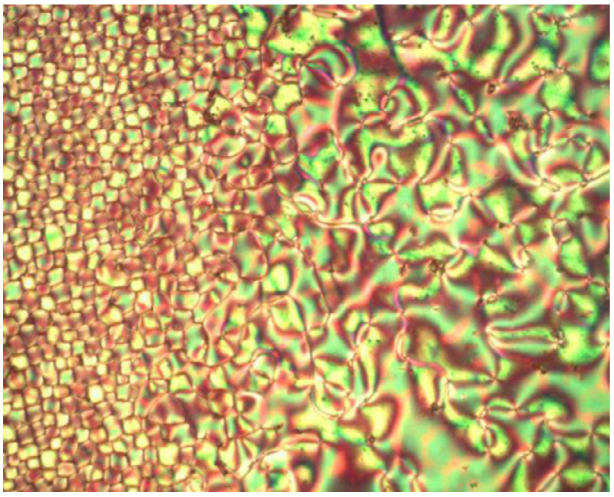

Fig. 4. Cross polarizing photomicrograph (×200) of complex $[Zn_2(L)(Q)_4]$ thread-like and nematic droplets texture near the isotropic of the nematic mesophase at 435 °C on heating.

complexes $[Mn_2(L)(Q)_4]$, $[Fe_2(L)(Q)_4]$ and $[Ni_2(L)(Q)_4]$ didn't showed any liquid crystalline behavior.

Appendix A. Supplementary data

Supplementary data associated with this article can be found, in the online version, at http://dx.doi.org/10.1016/j.ica.2017.07.029.

References

[1] S.J. Hsu, K.M. Hsu, M.K. Leong, I.J.B. Lin, Au(I)-benzimidazole/imidazole complexes. Liquid crystals and nanomaterials, Dalton Trans. 14 (2008) 1924–1931.
[2] H. Kima, Y. Jeonga, Y. Leea, Synthesis and characterization of polymers based on benzimidazole segments for polymer solar cells, Mol. Crys. Liq. Cryst. 581 (1) (2013) 25–30.
[3] S. Pal, W.S. Wang, I.J.B. Lin, C.S. Lee, Benzene benzimidazole containing Pd(II) metallacycle: Synthesis, X-ray crystallographic characterization and its use as an efficient Suzuki coupling catalyst, J. Mol. Catal. A: Chem. 269 (2007) 197–203.
[4] P. Hao, S. Zhang, W.H. Sun, Q. Shi, S. Adewuyi, X. Lu, P. Li, Synthesis, characterization and ethylene oligomerization studies of nickel complexes bearing 2-benzimidazolyl pyridine derivatives, Organometallics 26 (2007) 2439–2446.
[5] M. Grimmett, in: O. Meth-Cohn, A. Katritzky (Eds.), Ring Syntheses Involving Formation of Two Bonds: [4 + 1] Fragments, Academic Press, London, 1997, pp. 63–102.
[6] D. Yang, D. Fokas, J. Li, L. Yu, C.M. Baldino, A versatile method for the synthesis of benzimidazoles from o-nitroanilines and aldehydes in one step via a reductive cyclization, Synthesis 1 (2005) 47–56.
[7] O. Ninán, R. Chareyron, O. Figuereidoand, J. Santiago, Benzimidazole-based liquid crystals, Rev. Soc. Quím Perú. 72 (2006) 178–186.
[8] M.K. Paul, G. Kalita, A.R. Laskar, T.D. Choudhury, N.V.S. Rao, Synthesis and mesomorphism of new chiral imines and copper(II) complexes, J. Mol. Struct. 1039 (2013) 219–226.
[9] S. Tan, B. Wei, T. Liang, X. Yanga, Y. Wu, Anhydrous proton conduction in liquid crystals containing benzimidazolemoieties, RSC Adv. 6 (2016) 34038–34042.
[10] B. Wei, S. Tan, T. Liang, S. Cao, Y. Wu, Synthesis, structural and electrochemical characterization of benzimidazole compounds exhibiting a smectic C liquid crystal phase, J. Mol. Struct. 1133 (2017) 392–397.

[11] K. Bahrami, M.M. Khodaei, F. Naali, Mild and highly efficient method for the synthesis of 2-arylbenzimidazoles and 2-arylbenzothiazoles, J. Org. Chem. 73 (2008) 6835–6837.
[12] J.L. Serrano, Metallomesogens: Synthesis, Properties and Applications, VCH, Weinheim, Germany, 1996.
[13] S.R. Collinson, D.W. Bruce, in: J.P. Sauvage (Ed.), Transition Metals in Supramolecular Chemistry, Wiley, New York, 1999, pp. 285–369. Chapter 7.
[14] A.M. Giroud-Godquin, P.M. Maitlis, Metallomesogens: Metal complexces in organized fluid phases, Angew. Chem. Int. Ed. Engl. 30 (1991) 375–403.
[15] S.A. Hudson, P.M. Maitlis, Calamitic metallomesogens: metal-containing liquid crystals with rod like shapes, Chem. Rev. 93 (1993) 861–885.
[16] A. Santoro, A.M. Prokhorov, V.N. Kozhevnikov, A.C. Whitwood, B. Donnio, J.A.G. Williams, D.W. Bruce, Emissive metallomesogens based on 2-phenylpyridine complexes of iridium(III), J. Am. Chem. Soc. 133 (2011) 5248–5251.
[17] S.Y. Li, C.J. Chen, P.Y. Lo, H.S. Sheu, G.H. Lee, C.K. Lai, H-Bonded metallomesogens derived from salicyladiminates, Tetrahedron 66 (2010) 6101.
[18] O.N. Kadkin, J. An, H. Han, Y.G. Galyametdinov, A novel series of heteropolynuclear metallomesogens: organopalladium complexes with ferrocenophane-containing ligands, Eur. J. Inorg. Chem. 10 (2008) 1682–1688.
[19] A.K. Singh, S. Kumari, T.R. Rao, Microwave sintering of calcium phosphate ceramics, Mater. Sci. Eng., C 29 (2011) 1144.
[20] J.L. Serrano, T. Sierra, Helical supramolecular organizations from metal-organic liquid crystals, Coord. Chem. Rev. 242 (2003) 73–85.
[21] C.H. Lin, H.C. Kao, W.T. Sung, Y.W. Cheng, W.J. Wang, Cubic phase formation from new hexacatenar metallomesogens based on cobalt 3,4,5-trialkoxybenzoate, J. Chin. Chem. Soc. 62 (2015) 26–32.
[22] S. Maksym, M.M. Carmen, K. Vadim, G. Philipp, G. Yury, R. Jose, A. Spin crossover star-shaped metallomesogens of iron(II), Inorg. Chem. 53 (16) (2014) 8442–8454.
[23] D. Pucci, I. Aiello, A. Bellusci, A. Crispini, I.D. Franco, M. Ghedini, M.L. Deda, A "jellyfish" shaped green emitting gallium(III)-containing metallomesogen, Chem. Commun. 19 (2008) 2254–2256.
[24] N.N. Al-Mohammed, Y. Alias, Z. Abdullah, R.M. Shakir, E.M. Taha, A.A. Hamid, Synthesis and antibacterial evaluation of some novel imidazole and benzimidazole sulfonamides, Molecules 18 (2013) 11978–11995.
[25] L. Zhang, X. Chen, F. Zhao, X. Fan, P. Chen, Z. An, Synthesis and mesomorphic properties of 2-(4′- alkoxybiphenyl-4-yl)-1H-benzimidazole derivatives, Liq. Cryst. 40 (2003) 396–410.
[26] B. Kahveci, N. Karaali, F. Yilmaz, E. Mentes¸, An efficient synthesis of some new bisbenzimidazoles via microwave technique, Turkish J. Chem. 38 (2014) 423–429.
[27] W.J. Geary, The use of conductivity measurements in organic solvents for the characterization of coordination compounds, Coord. Chem. Rev. 7 (1) (1971) 81–122.
[28] A.Z. El-Sonbati, A.A. El-Bindary, Stereochemistry of new nitrogen containing aldehydes V. Novel synthesis and spectroscopic studies of some quinoline Schiff bases complexes, Polish Chem. 74 (2000) 621–630.
[29] K. Nakamoto, Infrared and Raman Spectra of Inorganic and Coordination Compounds, fourth ed., Wiley, New York, 1986.
[30] S. George, Infrared and Raman Characteristic Group Frequencies Tables and Charts, third ed., Wiley, New York, 2001.
[31] A.B.P. Lever, Inorganic Electronic Spectroscopy, first ed., Elsevier, London, 1968, pp. 267–355.
[32] R.L. Dutta, A. Syamal, Elements of Magnatochemistry, second ed., East West press, New Delhi, 1996.
[33] W. Manch, W. ConardFernelius, The structure and spectra of Nickel(II) and Copper(II) complexes, J. Chem. Edu. 38 (4) (1961) 192–201.
[34] M.A. Qaddoura, K.D. Belfield, Probing the texture of the calamitic liquid crystalline dimer of 4-(4-pentenyloxy)benzoic acid, Materials 3 (2010) 827–840.